MISSILE BASE FLOW: HYBRID RANS/LES COMPUTATIONAL FLUID DYNAMICS COMPARISONS TO MEASUREMENTS

K.D. Kennedy, C.D. Mikkelsen, AND B.J. Walker
U.S. Army AMRDEC Command
Redstone Arsenal, AL 35898

ABSTRACT

Combined Computational Fluid Dynamics Reynolds Averaged Navier-Stokes and LES model calculations were completed for comparisons with wind tunnel measurements of flow along the afterbody and in the base region of a circular cylinder aligned to a Mach 2.5 freestream. This cylinder is representative of a missile at zero degrees angle-of-attack. Comparison data includes afterbody and base pressure, high quality non-intrusive Laser Doppler Velocimetry and Pressure Sensitive Paint measurements, and turbulent kinetic energy.

1. INTRODUCTION

The flow in the base/separated region of a tactical missile is very complex even though the geometry is quite simple. There are several reasons this is the case. First, the external flow over the missile body is supersonic while the flow in the base region is mixed supersonic/subsonic flow. Second, this flow is characterized by shock wave/boundary layer interactions at the lip of the base region. Third, the flow is turbulent in the base/separated region and highly transient in nature.

There has been a long history of attempts to accurately describe this flow going back to the 1950's where integral models were used and continuing to the 2000's where sophisticated computation fluid dynamic models were used. However, none of these models have produced results that provide accurate descriptions of the flowfield.

Due to the technological advances that have been made in recent years in the field of Large Eddy Simulation (LES), parallel processing methods, and high speed computers, it was determined that it was time to make another attempt to solve these elusive problems.

Quality data sets extending from the early measurements of Reid and Hastings[1] through the JANNAF series[2,3] and the more recent measurements by Dutton and students[4-11] have consistently challenged the computational capability of the fluid dynamics community and even the recent calculations by Papp and Ghia[12] show disappointing comparisons with the cylindrical blunt base data of Herrin and Dutton[6]. Additional work using more advanced turbulence models (EASM, LES) by Ayyalasomayajula [13, 14] also failed to show improvement in the comparisons.

The objective of this work, then, is to determine if recent improvements to the Hybrid/RANS/LES AMRDEC CFD flow field model calculations show any better agreement with the UIUC LDV measurements. Of interest is the visualization of the flow field about a cylindrical body at 0 degrees angle-of-attack, surface pressure along the after body and base surfaces, and the flow field properties in the base region. A significant addition to these comparisons is the inclusion of the entire wind tunnel facility in the calculational domain since small-scale facilities can affect the results due to flow interactions with the facility geometry.

2. EXPERIMENTAL FACILITY

The experimental data described herein were collected in the Gas Dynamics Laboratory at the University of Illinois at Urbana-Champaign. This axi-symmetric wind tunnel facility was specifically constructed for the investigation of base flow phenomena. A photograph of the wind tunnel is shown in Figure 1. High pressure dry air, as illustrated in Figure 2, enters the stagnation chamber from a regulated supply, passes through a honeycomb flow-straightening module, and expands through a converging-diverging nozzle with central sting to an inviscid Mach number of 2.5 (actual measurements indicate a freestream Mach number of 2.46). This uniform supersonic flow (to within 1%) then passes through a test section and supersonic diffuser to exit the facility.

Report Documentation Page

Form Approved
OMB No. 0704-0188

Public reporting burden for the collection of information is estimated to average 1 hour per response, including the time for reviewing instructions, searching existing data sources, gathering and maintaining the data needed, and completing and reviewing the collection of information. Send comments regarding this burden estimate or any other aspect of this collection of information, including suggestions for reducing this burden, to Washington Headquarters Services, Directorate for Information Operations and Reports, 1215 Jefferson Davis Highway, Suite 1204, Arlington VA 22202-4302. Respondents should be aware that notwithstanding any other provision of law, no person shall be subject to a penalty for failing to comply with a collection of information if it does not display a currently valid OMB control number.

1. REPORT DATE	2. REPORT TYPE	3. DATES COVERED
DEC 2008	**N/A**	**-**

4. TITLE AND SUBTITLE **Missile Base Flow: Hybrid Rans/Les Computational Fluid Dynamics Comparisons To Measurements**	5a. CONTRACT NUMBER 5b. GRANT NUMBER 5c. PROGRAM ELEMENT NUMBER
6. AUTHOR(S)	5d. PROJECT NUMBER 5e. TASK NUMBER 5f. WORK UNIT NUMBER
7. PERFORMING ORGANIZATION NAME(S) AND ADDRESS(ES) **U.S. Army AMRDEC Command Redstone Arsenal, AL 35898**	8. PERFORMING ORGANIZATION REPORT NUMBER
9. SPONSORING/MONITORING AGENCY NAME(S) AND ADDRESS(ES)	10. SPONSOR/MONITOR'S ACRONYM(S) 11. SPONSOR/MONITOR'S REPORT NUMBER(S)

12. DISTRIBUTION/AVAILABILITY STATEMENT
Approved for public release, distribution unlimited

13. SUPPLEMENTARY NOTES
See also ADM002187. Proceedings of the Army Science Conference (26th) Held in Orlando, Florida on 1-4 December 2008, The original document contains color images.

14. ABSTRACT

15. SUBJECT TERMS

16. SECURITY CLASSIFICATION OF:			17. LIMITATION OF ABSTRACT	18. NUMBER OF PAGES	19a. NAME OF RESPONSIBLE PERSON
a. REPORT	b. ABSTRACT	c. THIS PAGE			
unclassified	**unclassified**	**unclassified**	**UU**	**7**	

Standard Form 298 (Rev. 8-98)
Prescribed by ANSI Std Z39-18

The objective of these tests was to simulate base flow about a missile at zero degree angle-of-attack. A cylindrical base configuration was fabricated from stainless steel and was mounted centrally through the wind tunnel nozzle. A schematic of the afterbody and flowfield is shown in Figure 2.

The test section, essentially a box to mount four flat optical windows for optical access, forms very complex recirculating cavity flows, which are quite difficult to model. However, according to Dutton, it was found that adjusting the stagnation pressure such that the nozzle exit lip pressure matched the pressure in the test cell could reduce waves that emanate from the nozzle exit lip which disrupt the near-wake flowfield. Under these conditions, interference waves, as viewed in Schlieren imagery (fig. 3), were seen to vanish at the matched pressure condition. Full details of the wind tunnel and model construction, as well as the LDV measurements, are given in References 15 and 16.

3. COMPUTATION METHODOLOGY

The AMRDEC CFD models the full Navier-Stokes (FNS) equation set providing an aero-thermo-chemical plume / airframe predictions for unsteady-flows[17]. The CFD code numerics include 1D/2D/Axi/3D finite volume discretization with an implicit, higher-order upwind (Roe/TVD) formulation (2nd order for RANS and 5th order for LES). The turbulence model includes a k-ε formulation with compressibility/vortical upgrades over standard models and includes several low R_e near-wall formulations. A variable, one/two equation Prandtl number/Schmidt model has been recently added. All equations are solved either fully implicitly or loosely coupled.

This Reynolds averaged code has been extended to handle three types of LES modeling. The first is Miles/LES that has no subgrid or wall modeling capability, the second is a Wall Blended/LES model that uses a hyperbolic blending function between RANS and LES near walls and the third model is a point-by-point Hybrid RANS/LES model (AJ). This AJ model alters from pure energy transferring (LES) to energy extracting (RANS) through a point-by-point blending function. The RANS solution provides a coarse limit of the LES solution. This hybrid model estimates the local range of scales before applying the blending via two additional equations. The first equation estimates the extent of unresolved flow and the second equation estimates the largest length scale of the flow. These two equations are similar in form to the RANS k-ε formulation but have different meanings. At each point in the flow, the RANS and LES viscosity is computed. A blending function that is based on the cell's location (i.e. wall boundary layer, shear layer, free stream, or mixed condition) is than used to compute the local viscosity.

Boundary conditions for this after body/base flow problem were specified as follows. Uniform subsonic conditions were fixed at the stagnation chamber inflow boundary for total conditions of 517 kPa pressure and 293 K. Gradient extrapolation procedures were used at the outflow boundary. Surface wall conditions were viscous with imposed adiabatic no slip flow. Boundary layers were grid resolved to < 1 Y+ using a So-Zhang-Speziale wall model. For comparison, RANS only calculations reset both the turbulent kinetic energy and production of turbulence values to chamber background values.

Several numerical grids were developed to take advantage of the symmetry of the wind tunnel configuration. This included the use of a pie shaped grid defining the stagnation chamber, throat, nozzle, and center sting. This pie wedge is then imposed onto a full 360 degree multi-block (interface) grid just upstream of the test section to allow for any possible downstream flow feed-back. The remaining grid is used to model the test section. The test section is modeled without walls - just outflow boundaries.

4. RESULTS AND DISCUSSION

Three different grid types were used to compute the solutions for comparison with data. The first grid included a full 360 degree region from chamber to test section and had 2.6 million points with one point every 3 degree circumferential angle. The second grid also included a full 360 degree region from chamber to test section and had 9.2 million points with one point every 1.5 degree circumferential angle. The third grid made use to the "pie wedge" grid mentioned above to model the chamber through nozzle region. This grid had a total 5.4 million points but due to the large grid point savings around the center sting, this grid had the most points in the base and downstream shear layer.

Using the three grids with the three different LES models produced the following results:

1) For base pressure, only the AJ model gave a near constant base pressure profile as shown in the comparison with measurements (fig. 4). Grid size was more important than LES model selection in terms of base pressure correlation. The best base pressure comparison results were produced using the AJ model run with 5.4 million grid points. The error was +6%. All other models produced results where base pressures were below the measured pressures and ranged in error by as much as -25%. The Miles case was the most numerically stable run (highest stable time step) while the wall-blended model was the least stable.

2) Centerline Turbulent Kinetic Energy (TKE) predictions varied greatly from the measured values (fig. 5). The 9.2 million grid case gave the best results. This figure shows that the measured TKE values on the centerline do not vary greatly over all axial locations (5000 to 7500 m^2/s^2). However, measured off-axis values are much higher.

3) For the centerline axial velocity, all models predicted the same axial profile shape except for the Miles model with 2.6 million grid points case (fig. 6). Most models predicted the zero velocity point downstream of measured point and most models predicted a larger negative axial velocity component in the recirculation zone.

4) No radial fluctuations were evident along the centerline, however the wall blended model predicted some noise near the base face. The measured data recorded a variation in radial velocity on the centerline of -10 to +20 m/s (fig. 7).

Axial/radial velocity and TKE measurements off the centerline were compared in detail with the AJ model using 5.4 million grid points (figs. 8-11). The axial velocity comparison clearly shows a much longer base flow region than measured. The radial velocity prediction compares well with the measurements. The velocity vector plot clearly shows the predicted base region (as defined by the zero velocity line) as larger and longer than measured. The TKE measurements show a much lower value over the region of the base flow. The predicted mixing layer profile clearly does not match the measured shear layer.

Looking to improve the modeled solution, it was thought that the tunnel walls might impact the base flow. An axisymmetric RANS case was run with and without the presence of the tunnel walls (for this case the windows were not modeled). The measured base pressure ratio was was found to average 0.56 P/P_{inf}. For the case where the walls were not modeled, the RANS normalized predicted base pressure was found to be 0.41 P/P_{inf} (-27% error). For the case where the walls were modeled, the RANS predicted base pressure was found to be 0.54 P/P_{inf} (-4% error) - a significant improvement. Clearly, the presence of the tunnel walls affects the axisymmetric RANS solution. The effects of the tunnel walls on a LES prediction were not addressed in this study.

5. SUMMARY AND CONCLUSIONS

Inclusion of the tunnel geometry improves the agreement with data.

1. The AJ RANS/LES point-by-point modeling gave the best base pressure results. The model, however, did an inadequate job of predicting the size and extent of the downstream base flow. This model needs more work.

2. The gross features of base flow phenomena are correct but local features differ significantly from the experimental measurements. LES predictions for base pressure are sensitive to both the model and grid points.

3. RANS/LES wall blended modeling is presently inadequate. The current hyperbolic wall blending function between full RANS and full LES is not physical.

4. Miles/LES modeling of the cylindrical base is inadequate. It is not meant for and should not be used for base flows where boundary layers are present.

Overall:

It appears that the model does not contain sufficient physics to handle the shock wave/boundary layer interactions that are predominant in the base flow cases studied.

REFERENCES

1. Reid, J., and Hastings, R.C., "The Effect of a Central Jet on the Base Pressure of a Cylindrical Afterbody in a Supersonic Stream," Aeronautical Research Council R&M No. 3224, December 1959.

2. Petrie, H., and Walker, B.J., "Tactical Missile Base Flow Investigation," Proceedings of the 15th JANNAF Exhaust Plume Technology Meeting, Ft. Sam Houston, Texas, 1985.

3. Petrie, H.L., and Walker, B.J., "Comparison of Experiment and Computation for a Missile Base Region Flowfield with a Centered Propulsive Jet," AIAA 1618, AIAA 18th Fluid Dynamics and Plasmadynamics and Lasers Conference, 16 July 1985, Cincinnati, Ohio.

4. Molezzi, M.J. and Dutton, J.C., "Study of the Near Wake Structure of a Subsonic Base Cavity Flowfield Using PIV", AIAA 3040, AIAA 24th Fluid Dynamics Conference, 6 July1993, Orlando, Florida.

5. Molezzi, M.J. and Dutton, J.C., "Application of Particle Image Velocimetry in High Speed Separated Flows," AIAA Journal, 31(3):438-446 (1993).

6. Herrin, J.L., and Dutton, J.C., "Supersonic Base Flow Experiments in the Near Wake of a Cylindrical Afterbody," AIAA Journal, 32(1):77-83 (1994).

7. Herrin, J.L., and Dutton, J.C., "Supersonic Near Wake Afterbody Boat Tailing Effects on Axisymmetric Bodies," Journal of Spacecraft and Rockets, 31(6):1021-1028 (1994).

8. Mathur, T., and Dutton, J.C., "Base Bleed Experiments with a Cylindrical Afterbody in Supersonic Flow," Journal of Spacecraft and Rockets, 33(1):30-37 (1996).

9. Mathur, T., and Dutton, J.C., "Velocity and Turbulence Measurements in a Supersonic Base Flow with Mass Bleed," AIAA Journal, 34(6):1153-1159 (1996).

10. Herrin, J.L., and Dutton, J.C., "The Turbulence Structure of a Reattaching Axisymmetric Compressible Free Shear Layer," Physics of Fluids, 9(11):3502-3512 (1997).

11. Bourdon, C.J., and Dutton, J.C., "Planar Visualizations of Large Scale Turbulent Structures in Axisymmetric Supersonic Separated Flows," Physics of Fluids, 11(1):201-213 (1999).

12. Papp, J.L., and Ghia, K.N., "Application of the RNG Turbulence Model to the Simulation of Axisymmetric Supersonic Separated Base Flows," AIAA-2001-0727.

13. Ayyalasomayajula, H., Kenzakowski, D. C., Papp, J. L., and Dash, S. M., "Assessment of k-e / EASM Turbulence Model Upgrades for Analyzing High Speed Aeropropulsive Flows," AIAA-2005-1101, 43rd Aerospace Sciences Meeting and Exhibit, Jan. 10-13, 2005, Reno, Nevada.

14. Ayyalasomayajula, H., Arunajatesan, S., Kannepalli, C., and Sinha, N., "Large Eddy Simulation of a Supersonic Flow Over a Backward-Facing Step For Aero-Optical Analysis," AIAA-2006-1416.

15. Boswell, B.A., and Dutton, J.C., "Flow Visualizations and Measurements of a Three-Dimensional Supersonic Separated Flow," AIAA Journal, 39(1) 113-121 (2001).

16. Boswell, B.A., and Dutton, J.C., "Velocity Measurements in a Pressure-Driven Three-Dimensional Compressible Turbulent Boundary Layer," AIAA-2001-0883, 39th AIAA Aerospace Sciences Meeting and Exhibit, 8-11 January 2001, Reno, Nevada.

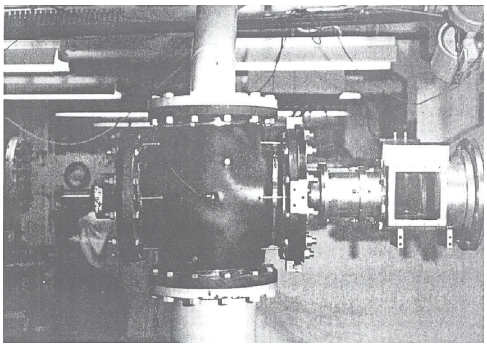

Figure 1. Wind Tunnel

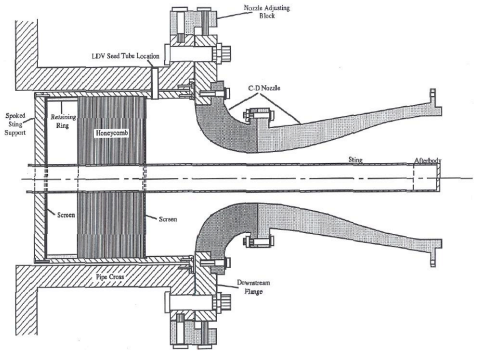

Figure 2. Wind Tunnel Setup

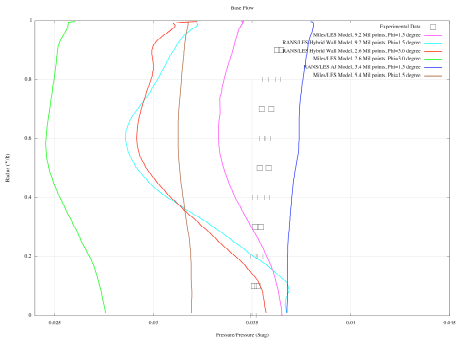

Figure 4. Base Pressure Comparison

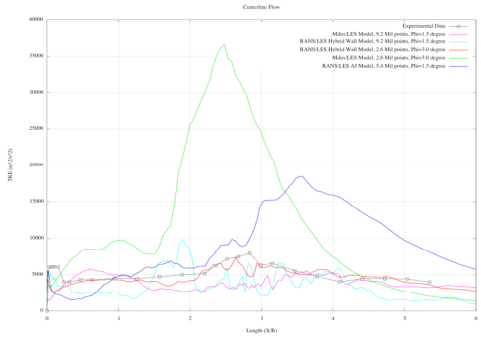

Figure 5. Centerline TKE Comparison

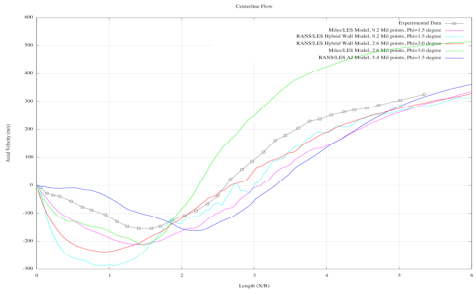

Figure 6. Centerline Axial Velocity

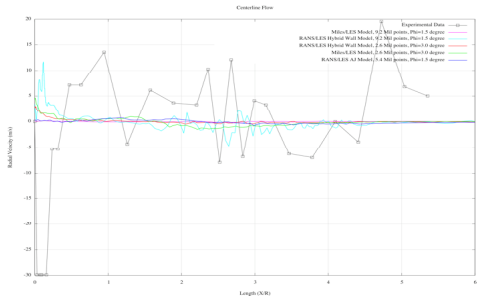

Figure 7. Centerline Radial Velocity

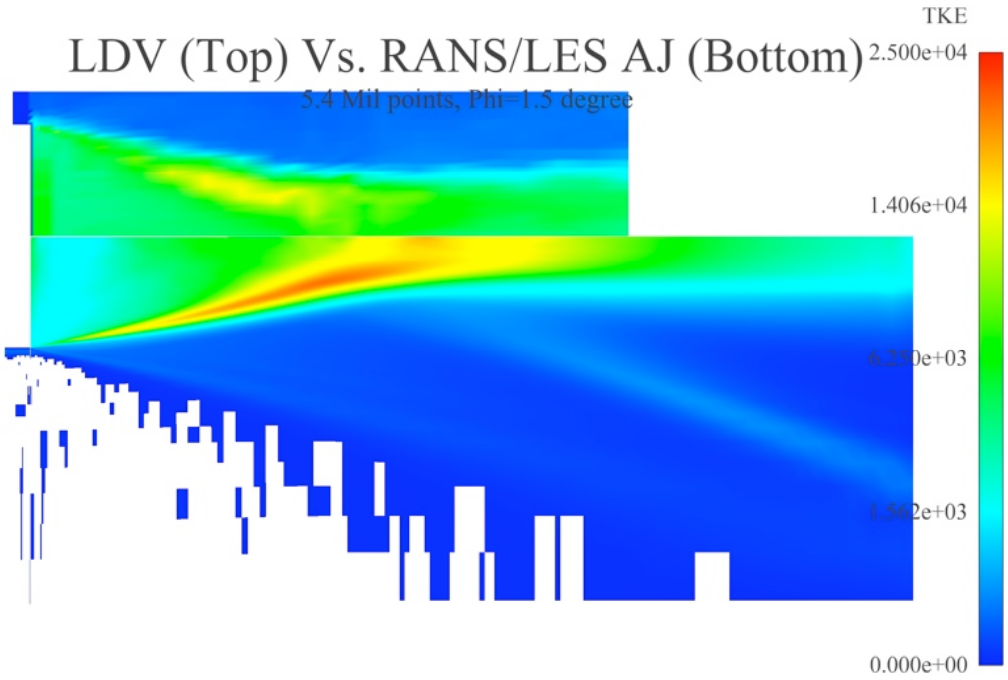

Figure 8. TKE Comparison to Measurements

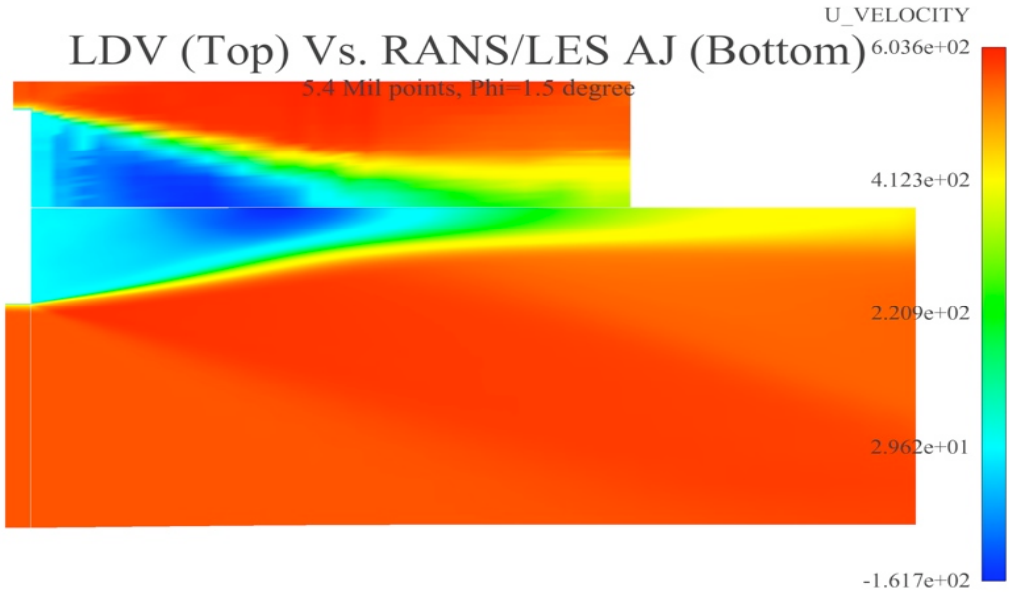

Figure 9. Axial Velocity Comparison to Measurements

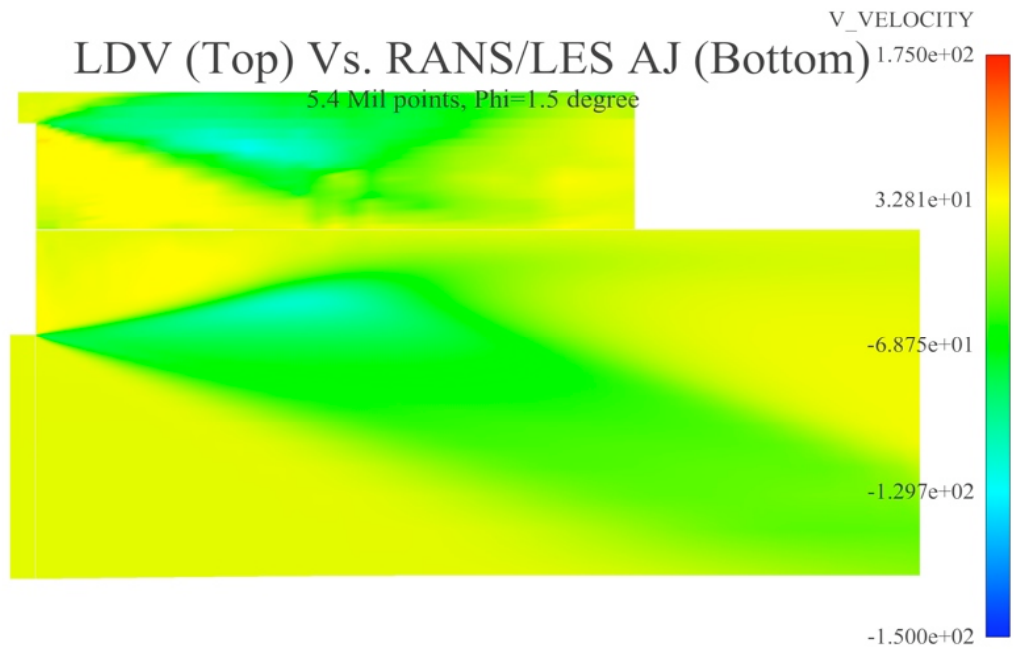

Figure 10. Radial Velocity Comparison to Measurements

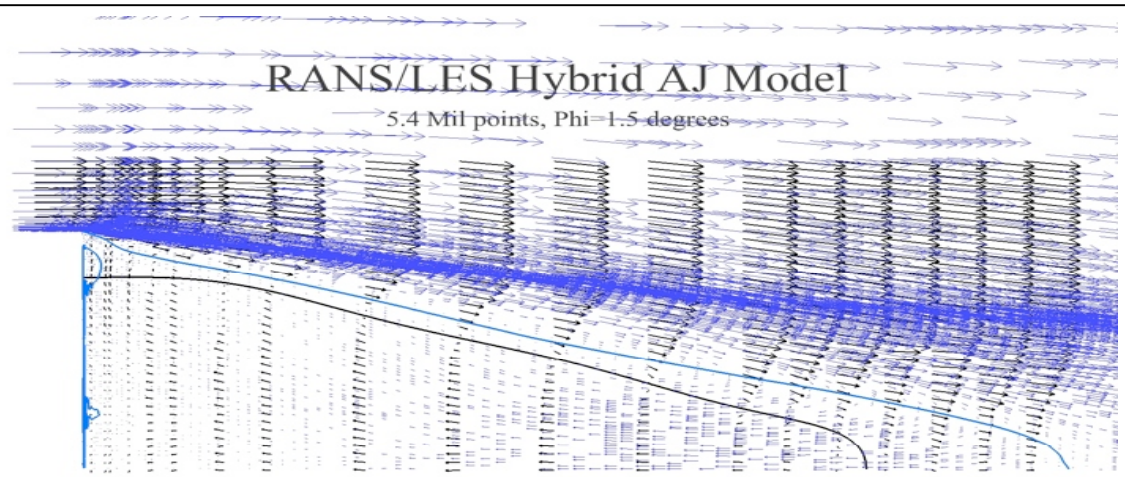

Figure 11. Vector Velocity Comparison to Measurements